



## Range measurements and thermal stability study of AZ111 photoresist implanted with Bi ions

R. B. Guimarães, L. Amaral, M. Behar, F. C. Zawislak, and D. Fink

Citation: *Journal of Applied Physics* **63**, 2502 (1988); doi: 10.1063/1.341029

View online: <http://dx.doi.org/10.1063/1.341029>

View Table of Contents: <http://scitation.aip.org/content/aip/journal/jap/63/8?ver=pdfcov>

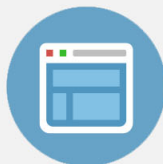
Published by the [AIP Publishing](#)

---



## Re-register for Table of Content Alerts

Create a profile.



Sign up today!



# Range measurements and thermal stability study of AZ111 photoresist implanted with Bi ions

R. B. Guimarães, L. Amaral, M. Behar, and F. C. Zawislak  
*Instituto de Física, Universidade Federal do Rio Grande do Sul, 90049 Porto Alegre, Brasil*

D. Fink  
*Hahn-Meitner-Institut, D 1000 Berlin 39, West Germany*

(Received 5 August 1987; accepted for publication 16 November 1987)

The Rutherford backscattering technique has been used to determine the range parameters of Bi ions implanted into AZ111 photoresist film at energies from 10 to 400 keV. An overall good agreement is found between the experimental results and the theoretical predictions by Biersack, Ziegler, and Littmark. It is also observed that a variation in the implantation dose does not affect the projected range and range straggling results, despite the fact that chemical modification of the implanted polymer layer is detected. In addition, we find that a shallow implantation of the polymer film with Bi ions increases the temperature at which the photoresist starts to decompose. Finally, at 300 °C the implanted Bi atoms diffuse preferentially toward the bulk. For this temperature, two different diffusion coefficients are estimated, one for the damaged region  $D_d = 1.2 \times 10^{-5}$  cm<sup>2</sup>/s and another for the bulk  $D_b = 1.2 \times 10^{-14}$  cm<sup>2</sup>/s.

## I. INTRODUCTION

The investigation of ion bombardment effects on polymers has received increased attention during the last years. Photoresists are currently used in the semiconductor industry as masking material during ion irradiation. Ion implantation can be applied to study the effects of radiation on the solubility, the thermal stability, and the electrical conductivity, as well as other physical properties of the polymers. In this framework, a considerable amount of work has been published and the results are summarized in several review papers.<sup>1,2</sup>

One of the less studied aspects of the ion implanted polymers is related to the characterization of the concentration profile of the implanted species. Despite the fact that projected ranges ( $R_p$ ) and projected range stragglings ( $\Delta R_p$ ) of implanted ions must be known to accurately determine the thickness of the masking films used in the fabrication of microelectronic devices, very few experimental profiles have been published. Several theoretical approaches can be used to calculate the ion implanted distribution parameters into polymers. Range codes which are available and suitable for multicomponent targets are the analytic code PRAL<sup>3</sup> and the Monte Carlo code TRIM.<sup>4</sup> They are conveniently summarized in the recent book of Ziegler, Biersack, and Littmark (ZBL).<sup>5</sup> The physical input into the range calculations consists of the new universal potential<sup>6</sup> and an improved electronic stopping power,<sup>5</sup> which is based on empirical proton stopping powers and on the concept of Brandt and Kitagawa<sup>7</sup> for heavy ions.

The work described here was undertaken with several aims. First, to test the ZBL predictions for complex targets, like a photoresist where there is a general lack of experimental data. Second, to study the influence of the implanted dose on the range parameters. It is known that high-dose implantation (typically  $\phi > 10^{14}$  ions/cm<sup>2</sup>) can modify the chemical composition of the implanted polymers.<sup>1,2</sup> Therefore, it is

important to examine how a change in the implanted dose can affect the characteristic parameters of the implanted profiles. Finally, we would like to study the thermal stability of the implanted polymers. It is known<sup>8</sup> that most of the photoresists remain stable up to 200 °C, but at higher temperatures they start to decompose losing O, H, and C. It appears worthwhile to look for possible effects of the ion implantation process on the thermal behavior of the photoresist, in particular, for changes in the decomposition dynamics as a function of temperature after implantation.

With the above purposes, we implanted <sup>209</sup>Bi into an AZ111 photoresist in the 10–400-keV energy range. The dose effect was studied at a fixed Bi implantation energy, by changing the total fluence from  $5 \times 10^{13}$  atm/cm<sup>2</sup> up to  $8 \times 10^{14}$  atm/cm<sup>2</sup>. Finally, we investigated the thermal behavior of the implanted polymer in the 30–400 °C range, the results being compared with the ones corresponding to an unimplanted sample. All the depth profile measurements were performed using the Rutherford backscattering (RBS) technique.

## II. EXPERIMENTAL PROCEDURE AND DATA ANALYSIS

Clean silicon wafers were spin coated with a AZ111 photoresist of thickness 1 μm and then baked for 1 h at 170 °C. Small pieces of the wafers ( $\cong 2$  cm<sup>2</sup>) were subsequently implanted with fluences and energies ranging from  $5 \times 10^{14}$  atm/cm<sup>2</sup> at 10 keV up to  $2 \times 10^{15}$  atm/cm<sup>2</sup> at 400 keV. For the study of the dependence of the range parameters on the implanted dose, five samples were implanted at an energy of 100 keV with doses ranging from  $5 \times 10^{13}$  atm/cm<sup>2</sup> up to  $8 \times 10^{14}$  atm/cm<sup>2</sup>. All the implantations were done at room temperature in the 400-keV ion implanter of the Institute of Physics, Porto Alegre. The beam current densities were  $\cong 50$  nA cm<sup>-2</sup> in order to avoid excessive heating of the samples.

Depth profiles were obtained via RBS analysis using

760–800-keV alpha particles from the same implanter. Each sample was measured twice with the beam impinging perpendicularly onto the sample's surface and under angles of 60°–70° with the sample's normal. The tilted geometry improves the depth resolution of the measurements. Back-scattered alpha particles were registered by a silicon surface-barrier detector placed at 160° with respect to the beam direction. The detection resolution of the system was better than 14 keV. The beam spot on the sample was changed whenever the  $\alpha$  dose reached the value of  $2 \times 10^{13}$  ions/cm<sup>2</sup> to avoid compaction effects and formation of carbon-rich regions as a consequence of large dose irradiation with the alpha beam. On the average, the total  $\alpha$  dose used to analyze each sample was around  $2 \times 10^{14}$  atm/cm<sup>2</sup>.

Data analysis was performed calculating directly from the measured spectra the four moments [ $R_p$ ,  $\Delta R_p$ ,  $\gamma$  (skewness), and  $\beta$  (kurtosis)] of the ion distribution. In all cases, the implanted profiles are Gaussian distributions with  $\gamma \cong 0$  and  $\beta \cong 3$ . The values of  $R_p$  and  $\Delta R_p$  have been determined by using the surface approximation with the  $\alpha$  particle stopping power taken from Ref. 5. Range stragglings have been calculated after deconvolution under the usual assumptions that the estimated energy straggling of the <sup>4</sup>He ions into the AZ111 photoresist and the system resolution are both Gaussians.<sup>9</sup> The main errors in the evaluation of the implanted profile are basically due to the uncertainty in the reported stopping powers which are around 5% (see, for example, Ref. 10), the instability of the electronic system and the lack of knowledge of the exact chemical composition of the photoresist.

### III. RESULTS

#### A. Dose effects

In order to see whether the profile parameters are dose dependent, we have implanted four AZ111 samples with total doses of  $5 \times 10^{13}$ ,  $10^{14}$ ,  $5 \times 10^{14}$ , and  $8 \times 10^{14}$  Bi/cm<sup>2</sup>, all at a fixed energy of 100 keV. Despite this wide range of the implanted dose, the Bi profiles remain basically the same. That is, they are Gaussian for all the samples, and the projected ranges and range stragglings are identical within the experimental errors, as is shown in Table I. This result is very important because for the lower implantation dose  $\phi < 10^{14}$  ions/cm<sup>2</sup>, no significant modifications in the chemical composition of the photoresist film has been detected as revealed by the corresponding RBS spectrum [see Fig. 1(a)]. On the contrary, for a dose of  $5 \times 10^{14}$  ions/cm<sup>2</sup>, we

TABLE I. Dose dependence of the range parameters of 100-keV <sup>209</sup>Bi implanted into 1- $\mu$ m film of AZ111. The estimated oxygen loss as a consequence of the implantation process, is also shown.

| Dose<br>( $10^{14}$ cm <sup>-2</sup> ) | $R_p$<br>(Å) | $\Delta R_p$<br>(Å) | Oxygen loss<br>(%) |
|--|--------------|---------------------|--------------------|
| 0.5                                    | 750          | 150                 | ...                |
| 1                                      | 780          | 155                 | ...                |
| 5                                      | 760          | 160                 | 20                 |
| 8                                      | 730          | 150                 | 35                 |

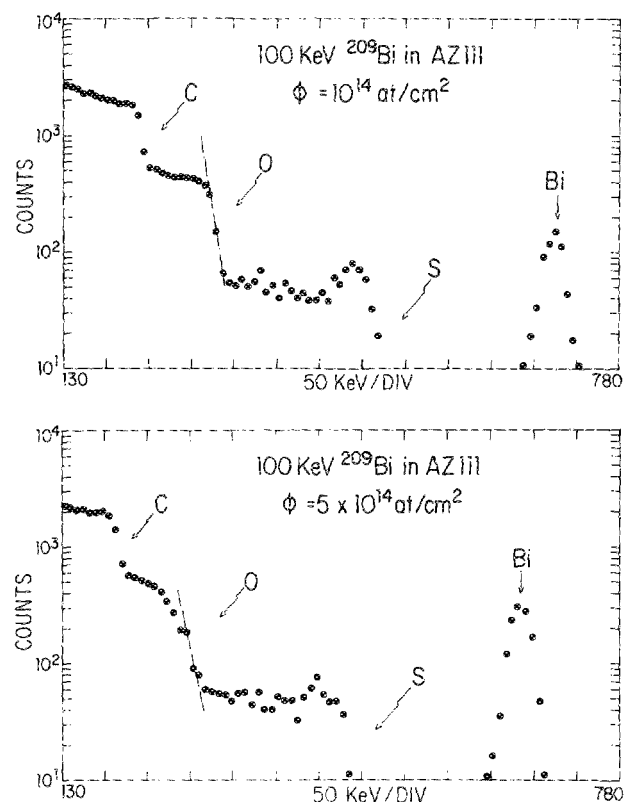


FIG. 1. (a) RBS spectrum of 100-keV Bi implanted into the AZ111 photoresist with a dose of  $10^{14}$  ions/cm<sup>2</sup>. No significant loss of oxygen and/or carbon is observed. (b) RBS spectrum of 100-keV Bi implanted into the AZ111 photoresist with a dose of  $5 \times 10^{14}$  ions/cm<sup>2</sup>. There is a loss of 20% of oxygen in the region from the surface up to 1300 Å.

have detected 20% of oxygen loss in the region from the surface up to 1300 Å as is shown in Fig. 1(b). The loss of oxygen increases for the larger implantation dose (see Table I). Nevertheless, the range parameters are rather insensitive to these chemical modifications.

In addition, for up to a total dose of  $4 \times 10^{14}$  He/cm<sup>2</sup>, the  $\alpha$  beam probe did not affect either the chemical composition of the AZ111 film or the range parameters of the implanted depth profiles. We have obtained the same results accumulating the  $\alpha$  beam dose in a single spot or frequently changing the position of the spot on the target. Despite this last result, we have analyzed our samples moving the position of the  $\alpha$  beam on the target, in order to avoid excessive local heating of the sample.

#### B. Range measurements

One of the major aims of the present work is to compare the experimental range parameters of Bi implanted into the AZ111 photoresist with the predictions by the ZBL theory.<sup>5</sup>

The universal potential and the improved electronic stopping power have been used as input to Monte Carlo simulation TRIM code program<sup>4</sup> (1986 version) in order to calculate the characteristic parameters of the ion distributions. The TRIM calculations further allow us to determine the higher moments of the range distributions. In the present case we have obtained  $\gamma = 0.06$ – $0.23$  and  $\beta = 2.95$  which,

TABLE II. Experimental and TRIM calculated projected ranges ( $R_p$ ) and range stragglings ( $\Delta R_p$ ) for  $^{209}\text{Bi}$  implanted into the AZ111 photoresist film.

| Energy (keV) | $R_p$ (exp) (Å) | $\Delta R_p$ (exp) (Å) | $R_p$ (TRIM) (Å) | $\Delta R_p$ (TRIM) (Å) |
|--------------|-----------------|------------------------|------------------|-------------------------|
| 10           | 180             | 31                     | 160              | 23                      |
| 20           | 240             | 36                     | 240              | 34                      |
| 30           | 310             | 50                     | 300              | 42                      |
| 50           | 450             | 72                     | 400              | 58                      |
| 70           | 550             | 100                    | 520              | 70                      |
| 100          | 750             | 140                    | 650              | 80                      |
| 200          | 1200            | 260                    | 1020             | 150                     |
| 400          | 2200            | 450                    | 1780             | 260                     |

after convolution with the experimental depth resolution function, give values of  $\gamma = 0.01$  to  $0.1$  and  $\beta \approx 2.9$  which are in quite good agreement with the results obtained in the present experiment ( $\gamma \approx 0$ ;  $\beta \approx 3$ ).

Table II shows the  $R_p$  and  $\Delta R_p$  experimental values as a function of the implanted energy together with the TRIM predictions. These results are also displayed in Fig. 2, where the continuous line shows the theoretical predictions as provided by the TRIM program. For energies up to 100 keV there is an overall good agreement (better than 8%) between the experimental and theoretical  $R_p$  values. However, at higher energies, the measured  $R_p$  are systematically higher than the theoretical ones, the difference being of the order of 25% at 400 keV. Regarding the  $\Delta R_p$  values we see the same behavior: There is good agreement between the predicted and measured values for low energy ( $E < 70$  keV) and increasing deviation at higher energies.

In our experimental range evaluation, as well as for the theoretical TRIM code calculations, we have used the density of the AZ111 films to be  $1.2 \text{ g/cm}^3$  as quoted by the supplier.<sup>11</sup> Also, for calculation purposes we have taken the nominal composition of the AZ111 photoresist to be  $\text{C}_5\text{H}_8\text{O}_2$ . It is important to mention that the relative difference between the theoretical and experimental  $R_p$  and  $\Delta R_p$  values is independent of the assumed photoresist density.

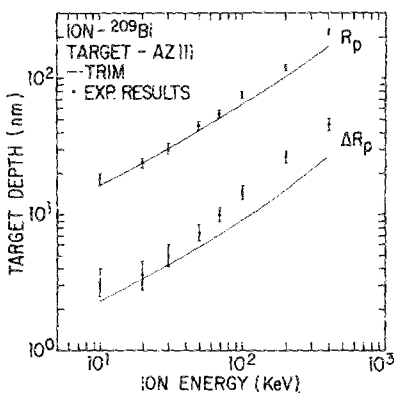


FIG. 2. Comparison of experimental and calculated projected range  $R_p$  and range straggling  $\Delta R_p$  as a function of energy. The points represent the experimental results. The full lines correspond to the theoretical TRIM predictions.

### C. Thermal stability

To investigate the influence of the ion implantation process on the thermal stability of the photoresist, we have performed isochronal annealings on both unimplanted and Bi 50-keV implanted samples, at 100, 200, 250, 300, and 350 °C for 20 min each in a vacuum better than  $10^{-6}$  Torr.

The RBS spectra of the unimplanted sample show that up to 200 °C, there is no significant change in the chemical composition of the photoresist. However, at higher temperatures the situation changes drastically as illustrated in Fig. 3. This figure shows the RBS spectra corresponding to the unannealed, annealed at 250 and 350 °C AZ111 polymer film. At 250 °C the RBS spectrum shows that there is a considerable and uniform loss of oxygen (around 30%), in all the observed depth from the surface up to 3000 Å. In addition, a small decrease in the C amount ( $< 15\%$ ) is also detected. At a higher temperature there is an increasing loss of material and finally at 350 °C, three main features can be observed: (i) the oxygen loss is around 50%; (ii) the C content of the sample is reduced in 25% and; (iii) the Si edge of the substrate appears in the RBS spectrum indicating that the film has become thinner (the thickness of the film at 350 °C is  $\approx 7500$  Å) as a consequence of the considerable loss of material.

On the other hand, the most important features of the thermal behavior of the implanted sample are shown in Fig. 4. Annealings up to 250 °C did not significantly change the photoresist composition nor the Bi depth profiles. Annealing at 300 °C results in the thermal diffusion of Bi, but still no major changes are detected in the AZ111 composition. Only at 350 °C does the RBS spectrum of Fig. 4 reveal an appreciable loss of oxygen and a drastic diffusion of the implanted Bi. Finally, at 400 °C the photoresist decomposes completely (not shown in the figure).

Furthermore, we studied the diffusion behavior of the implanted Bi into the AZ111 photoresist. Analysis of ther-

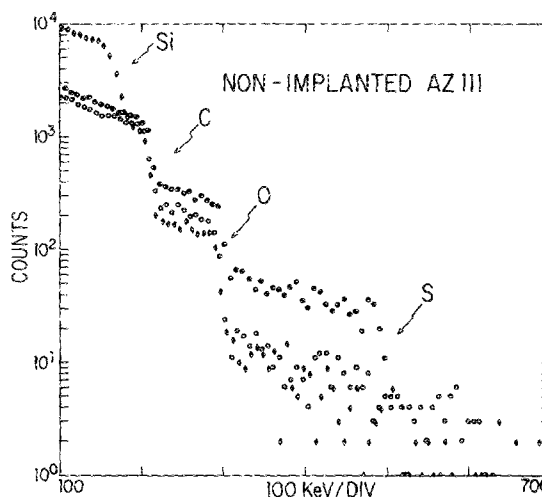


FIG. 3. RBS spectra corresponding to an unimplanted AZ111 polymer film: as received (full points); after 250 °C annealing (open points) and after 350 °C annealing (lozenge). After the last annealing there is an appreciable loss of material and as a consequence the film thickness is reduced in 25%, as can be deduced from the appearance of the Si substrate edge.

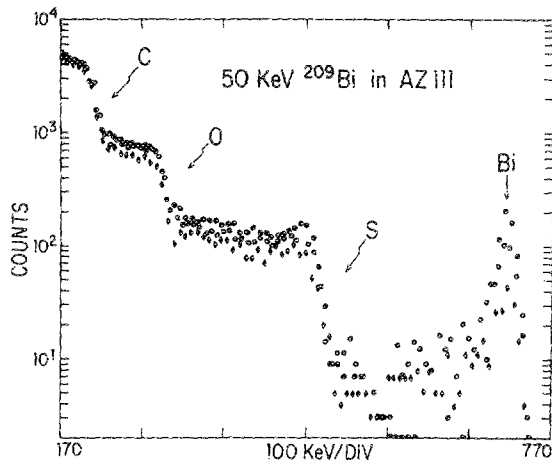


FIG. 4. RBS spectra corresponding to a shallow  $10^{14}$  Bi/cm<sup>2</sup> implantation into the polymer film: as-implanted (full points); after 300 °C annealing (open points) and after 350 °C annealing (lozenge).

mal diffusion experiments in implanted systems are difficult, essentially due to the damage produced by the implantation process, which does not always anneal out during or after the implantation, and affects the diffusion process here. To overcome these problems we analyzed our data with the numerical simulation method of "finite differences."<sup>12</sup> Earlier applications are given in Refs. 13 and 14. This technique calculates the diffusional change of any profile, channel by channel, and finally adds up all modified spectrum values. The diffusional change can be different for any channel, i.e., diffusion with depth dependent diffusion coefficients  $D(x)$  can be simulated. Furthermore, surface boundary effects as trapping and evaporation through the surface can be taken into account. Finally, it is possible to include trapping and detrapping probabilities  $A(x)$  and  $B(x)$  of the diffusing particle species at each channel. Alternatively, in case of non-zero detrapping probability, the hindered diffusion can be described by an effective diffusion constant

$$D_{\text{eff}}(x) = D(x) / [1 + A(x)/B(x)],$$

which makes the theoretical simulation process easier and more reliable, as the number of unknown variables is reduced. Therefore, this last procedure is applied here. For

convenience, we separate  $D(x)$  into a depth-independent value  $D^*$  and a normalized, dimensionless depth-dependent function  $f(x) = D(x)_{\text{eff}}/D^*$ .

Figure 5 shows the application of the above procedure. The full points represent the depth profile of Bi after 200 °C annealing (which is similar to the as-implanted one). The open points show the ion distribution after annealing at 300 °C. The insert in Fig. 5 displays the depth-dependent diffusion parameter used by the program in order to reproduce the final ion distribution profile.

According to TRIM calculations,<sup>4</sup> which predict that the damaged region should extend from the surface down to around 400 Å depth, we determined  $f(x)$  so that it is equal to 0.02 from surface to 400 Å depth, then increased linearly up to 0.22 at a depth of 700 Å, and maintains a constant value below. This procedure simulates a high trapping probability in the damaged region, and a very low one in the undamaged deeper zone, with a smooth transition between them. Furthermore, we assumed that the Bi could leave the photoresist and evaporate.

With these conditions, starting from the initial profile, after several iterations the program provides the depth profile shown in Fig. 5 as a full line. The agreement between the experimental result and the calculated one is quite satisfactory in particular, for the near surface (up to 450 Å) and bulk regions. The extracted diffusion coefficients for Bi in the damaged and bulk regions of the photoresist at 300 °C are, respectively,  $D_d = 1.2 \times 10^{-15}$  cm<sup>2</sup>/s and  $D_b = 1.2 \times 10^{-14}$  cm<sup>2</sup>/s.

#### IV. DISCUSSION AND CONCLUSIONS

It is well known that energetic ions damage and modify organic materials in a chemically irreversible fashion. Due to those radiation damage phenomena until recently, ion beam techniques have been largely overlooked in studying the properties of polymers and polymer structures. On the other hand, non-nuclear techniques give only very indirect depth profile information explaining the sparse data in the literature.

In this work we have shown conclusively, that range parameters describing implanted depth profiles of polymer layers are rather insensitive to the chemical modifications

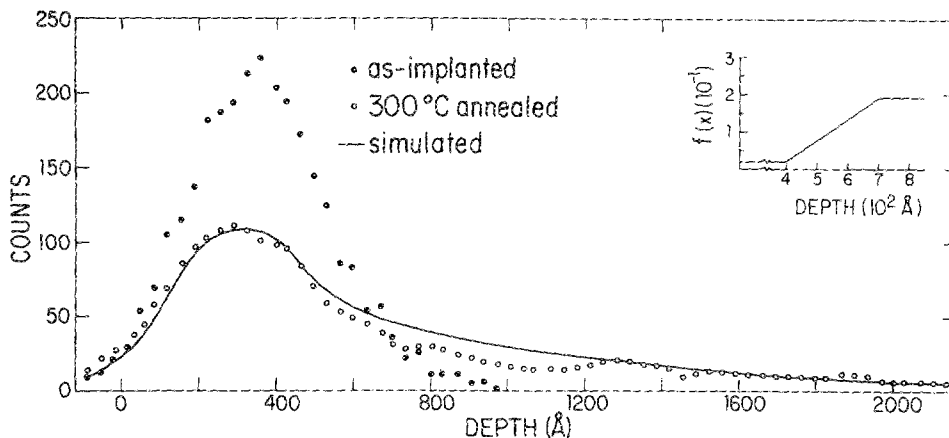


FIG. 5. Full points represent the Bi depth profile after 200 °C annealing. The open points show the ion distribution after annealing at 300 °C. The insert displays the depth dependent diffusion parameter used in the calculation. Smooth curve represents the simulated depth profile.

produced by the implantation process, despite the rather wide range of implanted doses. We have also demonstrated that the energetic  $\alpha$  probe beam neither significantly alters the chemical composition of the AZ1111 film (in a dose range compatible with the RBS profile measurements), nor affects the range parameters of the concentration profiles.

Concerning the range predictions of the ZBL theory, we can conclude that there is an overall good agreement between the calculated and experimental values. The discrepancies observed at higher energies (around 20% for  $R_p$  and 70% for  $\Delta R_p$ ) are beyond the experimental errors. The disagreement cannot be attributed to the lack of precise knowledge of the polymer's density, because the relative difference between the experimental and theoretical values is independent of the assumed density. On the other hand, for both the experimental and theoretical calculations we have taken the nominal composition of the polymer to be  $C_5H_8O_2$ . If the composition is different, variations in both experimental and theoretical range values are expected, which would be a source of the observed disagreement. We feel that further experimental work is needed in order to observe if the present discrepancies are characteristic of the Bi-AZ1111 system, or if some more general features are present, for example, the validity of the Bragg's rule, used for the evaluation of the experimental results, or the precision in the ZBL prediction for complex targets.

Concerning the thermal behavior of the implanted polymers, our results have clearly shown that as a consequence of the implantation process there is an increase in the temperature at which the photoresist starts to decompose. We have observed that the unimplanted sample starts to loose oxygen at around 200 °C, confirming previous experiments [see, for example, Ref. 8]. On the other hand a low-dose and shallow implantation of Bi raises the decomposition temperature of the AZ1111 polymer to 350 °C. A possible and very speculative explanation can be related to the fact that the Bi implantation creates damage and therefore inhibits the diffusion

process of the oxygen. This hypothesis is, in a way, confirmed by our thermal diffusion studies of the implanted Bi. As was mentioned above, we were able to estimate two diffusion coefficients, one for the damaged region and another for the bulk. They differ by one order of magnitude which may be attributed to the retarded diffusion which occurs due to damage produced by the implantation process. Therefore, one might conclude that both processes, the rising of the decomposition temperature of the polymer and the inhibited diffusion in the implanted region could be related to the same origin, the damage produced by the implantation process.

## ACKNOWLEDGMENT

We would like to acknowledge the helpful suggestions given by Dr. J. P. Biersack.

<sup>1</sup>T. Venkatesan, Nucl. Instrum. Methods B 7/8, 461 (1985).

<sup>2</sup>W. L. Brown, Radiat. Eff. 99, 281 (1987).

<sup>3</sup>J. P. Biersack, Z. Phys. A 305 95 (1982).

<sup>4</sup>J. P. Biersack and L. G. Haggmark, Nucl. Instrum. Methods 174, 257 (1980).

<sup>5</sup>J. P. Biersack and U. Littmark, in *Stopping and Ranges of Ions in Matter*, edited by J. F. Ziegler (Pergamon, New York, 1985), Vol. 1, p. 1.

<sup>6</sup>J. P. Biersack and J. F. Ziegler, in *Ion Implantation Techniques*, Vol. 10 of *Springer Series in Electrophysics*, edited by H. Ryssel and H. Glawischnig (Springer, Berlin, 1982), pp. 122-156; Nucl. Instrum. Methods 194, 93 (1982).

<sup>7</sup>W. Brand and M. Kitagawa, Phys. Rev. B 25, 5631 (1982).

<sup>8</sup>Y. Okuyama, T. Hashimoto, and T. Yoguchi, J. Electrochem. Soc. 125, 1293 (1978).

<sup>9</sup>W. Chu, J. W. Mayer, and M.-A. Nicolet, *Backscattering Spectroscopy* (Academic, New York, 1978).

<sup>10</sup>D. C. Sentry and R. D. Werner, Nucl. Instrum. Methods 178, 523 (1980).

<sup>11</sup>Shypley Co., Zürich, Switzerland.

<sup>12</sup>G. D. Smith, *Numerical Solution of Partial Differential Equations: Finite Difference Methods*, 2nd ed. (Clarendon, Oxford, 1978).

<sup>13</sup>J. P. Biersack and D. Fink, in *Ion Implantation into Semiconductors and Other Materials*, edited by T. Namba (Plenum, New York, 1975), p. 211.

<sup>14</sup>M. Behar, J. P. Biersack, P. F. P. Fichtner, D. Fink, C. A. Olivieri, and F. C. Zawislak, Nucl. Instrum. Methods B 14, 173 (1986).